Forbidden interval of propagation speed for exothermic chemical fronts

M. Leda,[1,2] A. Lemarchand,[1,*] and B. Nowakowski[2,3]
[1]*Université Pierre et Marie Curie - Paris 6, UMR 7600 LPTMC, F-75005 Paris, France and C.N.R.S. UMR 7600 LPTMC, F-75005 Paris, France*
[2]*Institute of Physical Chemistry, Polish Academy of Sciences, Kasprzaka 44/52, 01-224 Warsaw, Poland*
[3]*Physics Laboratory, Warsaw University of Agriculture, Nowoursynowska 159, 02-776 Warsaw, Poland*
(Received 8 December 2006; published 8 May 2007)

We consider the propagation of an exothermic chemical front toward an unstable steady state. The hydrodynamic equations are solved numerically for increasing values of the activation energy of the reaction which controls the reaction front speed. For a large speed, the marginal stability criterion of the isothermal case is recovered. For a small speed, we observe two well-separated traveling waves: a heat front is preceding the reaction front. We find analytically a forbidden speed interval where the hydrodynamical system does not admit stationary traveling solutions.

DOI: 10.1103/PhysRevE.75.056304 PACS number(s): 47.70.Fw, 47.70.Pq, 82.40.Ck

INTRODUCTION

Since the works of Fisher [1] and Kolmogorov *et al.* [2], the speed selection of reaction-diffusion fronts propagating into an unstable state has attracted considerable attention in the literature [3–5]. The macroscopic analysis of chemical wave fronts has been mainly devoted to the isothermal case, for which the marginal propagation velocity is selected. However, chemical reactions are usually exothermic and the concentration wave is then associated with thermal waves. The theory of flame propagation initiated by Frank-Kamenetskii [6] and Zel'dovich [7] is limited to the description of mass and heat diffusion processes [8]. In this frame, combustion of premixed gases has been extensively studied [7,9–11]. However, this approach fails here since the ratio of mass diffusivity and thermal diffusivity is close to unity.

In this paper, we perform the complete hydrodynamic description of an exothermic chemical wave front propagating in a gaseous medium. The reaction considered can be fast and is accompanied by a heat release, that is small compared to the thermal energy. The Fisher front is known to be sensitive to small perturbations occurring in the leading edge [4,12–19]. Macroscopic and microscopic results obtained for a single value of the reaction front velocity have been reported previously [20]. The objective of this paper is to examine the validity of the marginal stability criterion in the presence of a heat release. We study the different types of solutions obtained in a wide range of reaction front velocity and expect qualitatively different behaviors depending on the relative speed of the chemical front and the heat front.

First, the hydrodynamic equations governing the evolution of the exothermic Fisher front are numerically solved for increasing values of the activation energy of the reaction, leading to different reaction front speeds. Then we analytically prove the existence of a speed gap where traveling fronts are excluded.

*Author to whom correspondence should be addressed, Electronic address: anle@lptmc.jussieu.fr

HYDRODYNAMIC EQUATIONS

We consider a one-dimensional infinite medium initially divided into two adjacent parts filled with components A and B, respectively. At the chemical interface, the following exothermic reaction occurs:

$$A + B \rightarrow 2A + \text{heat } Q. \tag{1}$$

The heat release Q is small compared to k_BT, where k_B is the Boltzmann constant and T is the temperature. In the isothermal case $Q=0$, the total concentration ρ remains constant and the macroscopic evolution of the system is governed by a single reaction-diffusion equation for the local concentration a of species A. This equation admits a family of wave front solutions, moving at constant speed U and replacing the unstable $a=0$ stationary state by the stable $a=\rho$ stationary state. Steep initial profiles evolve to the marginally stable front [3] propagating with velocity $U_0=2\sqrt{k\rho d}$, where k is the rate constant of reaction (1) and d is the diffusion coefficient of species A and B.

In the case of the exothermic chemical reaction (1), the dynamics of the reactive gas is governed by four balance equations for total concentration $\rho(x,t)$, stream velocity $u(x,t)$, pressure $p(x,t)$, and concentration $a(x,t)$ of species A:

$$\partial_t\rho = -\partial_x(\rho u), \tag{2}$$

$$\partial_t u = -\frac{1}{m\rho}\partial_x\left(p - \frac{4}{3}\eta_0\sqrt{T}\partial_x u\right) - u\partial_x u, \tag{3}$$

$$\partial_t p = -\frac{2}{3}\left(p - \frac{4}{3}\eta_0\sqrt{T}\partial_x u\right)\partial_x u - \partial_x(pu) + f_0\partial_x(\sqrt{T}\partial_x T) + \frac{2}{3}QR, \tag{4}$$

$$\partial_t a = -\partial_x(au) + d_0\partial_x[\sqrt{T}\partial_x(a/\rho)] + R, \tag{5}$$

where the temperature obeys $T=p/(k_B\rho)$ for an ideal gas. We use the expressions of the transport coefficients for the hard sphere model with cross section σ and particle mass m [21,22]: $f_0\sqrt{T}=\frac{25k_B}{32\sigma}\sqrt{\frac{\pi k_BT}{m}}$ is the heat conductivity, d

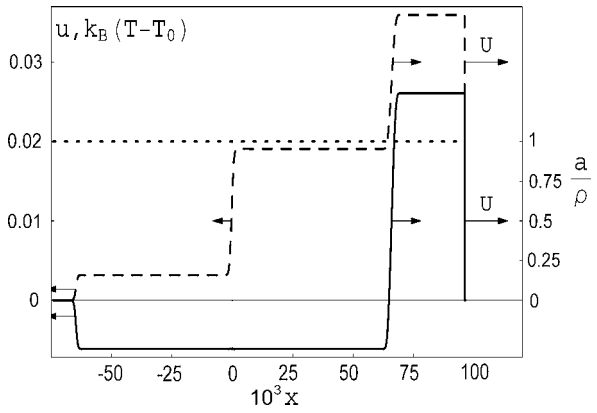

FIG. 1. Numerical solution to Eqs. (2)–(5) for $\sigma=0.007\,942\,201\,044\,98$, $Q=0.04k_BT_0$, $k_BT_0=1$, and $\epsilon=0.5$. Solid line corresponds to stream velocity u, dashed line to $k_B(T-T_0)$, and dotted line to reactive interface a/ρ.

$=d_0\sqrt{T}/\rho$ is the diffusion coefficient with $d_0=\frac{3}{8\sigma}\sqrt{\frac{\pi k_B}{m}}$, and $\eta_0\sqrt{T}=\frac{5}{12\sigma}\sqrt{\pi k_BTm}$ is the shear viscosity. The reactive term reads $R=ka(\rho-a)$ with $k=4\sigma\sqrt{\frac{k_BT}{\pi m}}\exp\left(-\frac{E_a}{k_BT}\right)$, where E_a is the activation energy of reaction (1).

Complete hydrodynamic descriptions of chemical systems have been performed for a linear consumption of the reactant [23,24]. We consider here a nonlinear reaction scheme for which traveling fronts exist even in the isothermal case. We solve numerically Eqs. (2)–(5) using the Euler method. Total concentration, stream velocity, and temperature are initially homogeneous and fixed at $\rho_0=20$ in arbitrary units, $u_0=0$ and $k_BT_0=1$, respectively. The initial concentration profile is a step function, with species A on the left ($x\leqslant 0$) and species B on the right ($x>0$). The heat of the reaction is fixed at $Q=0.04k_BT_0$. Due to the reaction, species B is transformed into A which expands to the right of the medium. The length is initially $L=400$. In order to mimic the propagation of the front in an infinite medium [14], we continuously check the values of the hydrodynamic variables in the boundary layers of length $L_b=50$ at the ends of the system. If the perturbation induced by the exothermic reaction reaches a boundary layer, we increase the system at this perturbed boundary by $\Delta L=1$. The transport coefficients are calculated for the cross section $\sigma=0.007\,942\,201\,044\,98$ and the particle mass $m=1$. For these values, the width of the reaction front in the isothermal case is equal to 75 for $E_a=2k_BT_0$, $\rho=\rho_0$, and $T=T_0$.

When the activation energy $\epsilon=E_a/k_BT_0$ increases, the reaction rate k decreases and we expect that the reaction front propagates more slowly. However, two qualitatively different types of solutions are obtained as the reaction front velocity decreases.

Figure 1 gives the profiles of the stream velocity u, the temperature T, and a/ρ, for a small value of the activation energy, $\epsilon=0.5$. After a transient, three steps appear on the profile of u and four steps appear on the profile of T. The profile of pressure p has a similar shape as the profile of u, and the total concentration ρ behaves like T. For this value of ϵ, the fastest front, connected with the single step of a/ρ, is the reaction interface. For the temperature profile, this interface is associated with the first front observed from the right.

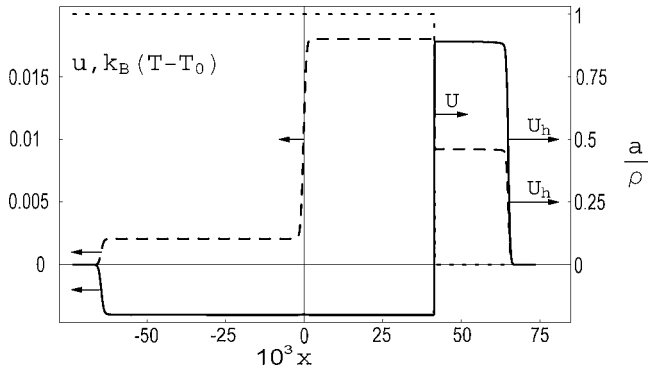

FIG. 2. Same caption as Fig. 1 but $\epsilon=2.25$.

The values of the variables behind the reaction front are greater than the values ahead of it. In particular, the stream velocity behind the reaction front is positive. The amplitude of all the variables are increasing with ϵ. The second step of the temperature profile is related to the heat propagation. It is not a stationary front: on the left plateau of the step the stream velocity u is negative, whereas it is positive on the right plateau, so that the width of this second step increases in time. These are the features of the solutions obtained for $\epsilon\leqslant 1.0$.

The results obtained for a larger activation energy, $\epsilon=2.25$, are given in Fig. 2. In this case, two stationary fronts propagate to the right: the first front corresponds to the heat propagation, whereas the second front corresponds to the reaction interface. The velocity U_h of the heat front is greater than the velocity U of the reaction front. The heat front moves to the unperturbed steady state (ρ_0, $u=0$, T_0, $a=0$) and the values of ρ, u, and p are greater behind it. The amplitudes of the heat front decrease with ϵ, which results in a decrease of its velocity. The values of ρ, u, and p behind the reaction front are smaller than ahead of it. This type of behavior is observed for $\epsilon\geqslant 1.7$.

In both ranges of activation energies the temperature profile possesses two other fronts that propagate to the left in the region containing only component A. The third traveling front moves in a region where u and p are constant: it moves with a small speed given by this constant negative stream velocity. The fourth front is a heat front which propagates to the unperturbed steady state (ρ_0, $u=0$, T_0, $a=\rho$).

A straightforward generalization of the expression of the marginal speed to an exothermic reaction leads to $U_0(T)=2\sqrt{k(T)\rho d(T)}$, where T is the temperature in the leading edge. Figure 3 gives the speed U of the reaction front vs the activation energy ϵ. The front speed can be defined in the two separated intervals of ϵ. In the range $\epsilon\leqslant 1.0$, the fast reaction front propagates toward the unperturbed steady state and the marginal velocity $U_0(T_0)$ gives a fairly good approximation to the front speed. In the second range, $\epsilon\geqslant 1.7$, positive deviations from the marginal speed $U_0(T_1)$ are observed, where T_1 is the value of the temperature ahead of the reaction front. They vanish as ϵ increases, because the perturbation induced by the heat front becomes smaller as it escapes more rapidly from the slower reaction interface.

In the intermediate range of activation energies, $\epsilon\in[1.1,1.65]$, the numerical calculations lead to nonstation-

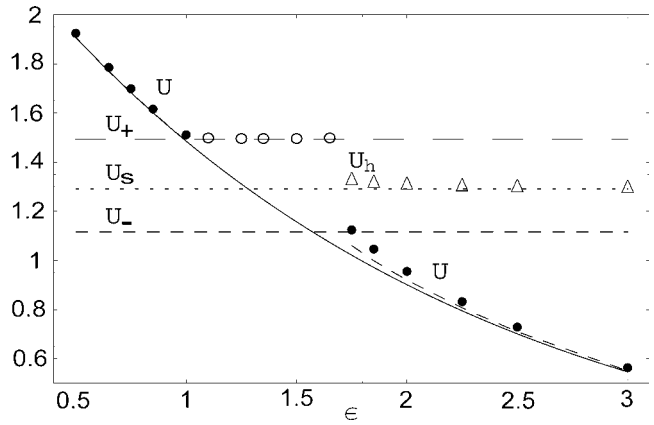

FIG. 3. Front velocities vs activation energy ϵ. Solid line and dashed line correspond to marginal velocity $U_0(T)$ of isothermal Fisher front for $T=T_0$ and $T=T_1$, respectively (T_1 is the value of temperature ahead of the numerically obtained reaction front). Solid circles corresponds to reaction front velocities obtained in numerical solution of Eqs. (2)–(5). Open circles give velocities of reacting interface for nonstationary solutions. Horizontal long-dashed line and short-dashed line give critical reaction front velocities U_+ and U_-, respectively. Horizontal dotted line gives sound speed U_s at T_0. Open triangles correspond to heat front velocities obtained in numerical solution of Eqs. (2)–(5).

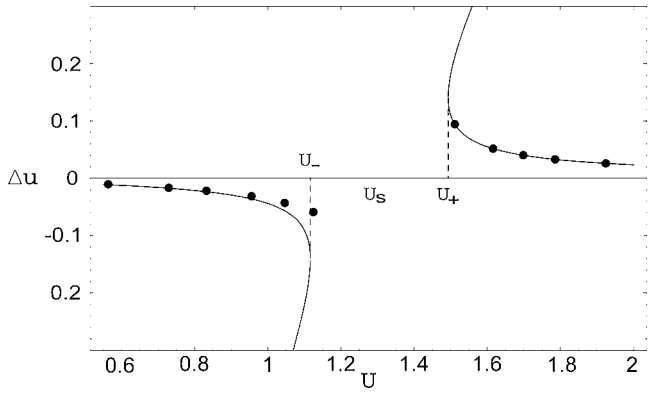

FIG. 4. Height Δu of stream velocity front corresponding to reaction front vs reaction front velocity U. Solid line gives solution to Eq. (9) for $T_1=T_0$ and $v_1=-U$. Solid circles correspond to numerical solution to Eqs. (2)–(5).

ary solutions. Due to the accumulation of heat in the reaction zone, peaks that broaden with time appear in the profiles of u, ρ, and T. However, the reactive interface a/ρ moves with a constant velocity that does not change with the activation energy and remains close to the value reached by the stationary front for $\epsilon=1.0$. We examine this phenomenon analytically in the next section.

TRAVELING FRONTS

We consider the stationary reaction fronts moving to the right at speed U. The values of the hydrodynamic variables on the plateaus associated with the front are denoted by ρ_i, u_i, p_i, and a_i, with $i=1$ ahead of the front and $i=2$ behind it. For the reaction front one has $a_2=\rho_2$. When we switch to the frame moving with the front, the stream velocity becomes $v=u-U$.

In the moving frame Eqs. (2)–(5) lead to the following Hugoniot relations [25,22]:

$$\rho_2 v_2 = \rho_1 v_1, \tag{6}$$

$$p_2 + m\rho_2 v_2^2 = p_1 + m\rho_1 v_1^2, \tag{7}$$

$$\frac{3}{2}k_B T_2 + \frac{m}{2}v_2^2 + \frac{p_2}{\rho_2} - Q = \frac{3}{2}k_B T_1 + \frac{m}{2}v_1^2 + \frac{p_1}{\rho_1}. \tag{8}$$

Then the height $\Delta u=v_2-v_1$ of the stream velocity obeys

$$4mv_1(\Delta u)^2 + (3m(v_1)^2 - 5T_1k_B)\Delta u + 2Qv_1 = 0. \tag{9}$$

This equation does not have real roots if $v_1 \in]v_{1+}, v_{1-}[$ where

$$v_{1\pm} = -\sqrt{\frac{15T_1k_B + 16Q \pm 4\sqrt{2Q(15T_1k_B + 8Q)}}{9m}}. \tag{10}$$

The solutions Δu of Eqs. (9) are negative if $v_1 < v_{1+}$ and positive if $v_1 > v_{1-}$.

We first apply these results to the reaction front propagating to the unperturbed steady state, i.e., for $u_1=0$, $T_1=T_0$, and $\Delta u=u_2$. The forbidden interval of stream velocities $]v_{1+}, v_{1-}[$ ahead of the front results in a forbidden interval of reaction front velocities $]U_-, U_+[$ where $U_-=-v_{1-}$ and $U_+=-v_{1+}$. Figure 4 presents the dependence of the height Δu of the stream velocity front vs the reaction front velocity U. The analytical solutions Δu of Eq. (9) for $U \geqslant U_+$ are compared to the values u_2 of the stream velocity behind the reaction front obtained when solving numerically Eqs. (2)–(5) for $\epsilon \leqslant 1$. In the case of the reaction front propagating behind the heat front, the values of v_1 and T_1 obtained numerically for $\epsilon \geqslant 1.7$ are introduced in Eq. (9). Then we are able to compare the solutions of Eq. (9) for $U \leqslant U_-$ with the numerical values of Δu. Using Eq. (10) for $T_1=T_0$, we find that the greater critical value of the reaction front velocity is $U_+ \approx 1.4932$. To compute the smaller critical value U_-, we assume $T_1 \approx T_0$ and $v_1 \approx -U$. It gives $U_- \approx 1.1161$. As shown in Fig. 4, the analytical results confirm the noncontinuous dependence of the height Δu on the reaction front velocity U.

It is noteworthy that in the intermediate range of activation energies, $\epsilon \in [1.1, 1.65]$, the propagation speed of the reactive interface, a/ρ, remains constant and close to U_+, as presented in Fig. 3.

We use the same approach to describe the heat front propagating ahead of the reaction front at velocity U_h. In this case, $Q=0$, $T_1=T_0$, $v_1=-U_h$ and Eq. (9) has always two real solutions given by

$$\Delta u = \frac{3mU_h^2 - 5T_0k_B}{4mU_h}, \quad \Delta u = 0. \tag{11}$$

The height Δu of the stream velocity front is positive for velocities $U_h > U_s$ where $U_s = \sqrt{5T_0k_B/3m}$ is the sound speed

at T_0. As shown in Fig. 3, the velocity of the heat front deduced from the numerical solutions of Eqs. (2)–(5) reaches U_s for large activation energies $\epsilon \geqslant 1.7$. The forbidden interval $]U_-, U_+[$ of reaction front velocities encloses the sound speed U_s.

For a small value of the reaction heat Q we have proven that stationary reaction fronts exist for either large or small propagation velocities. According to Eq. (10), the forbidden interval of reaction front speeds increases with Q so that stationary solutions exist only either for extremely fast reaction fronts or sufficiently slow fronts, i.e., large activation energies. Experimental validations could involve conformational isomers identified by their infrared spectra. The orders of magnitude of the activation energy and heat release are in the relevant range for the rotamers of protonated alanine dipeptide [26]. To investigate the behavior at higher Q's, the autocatalytic isomerization of *n*-butene into isobutene [27] could be considered. The knowledge of the specific chemical mechanism is not required: the invariants given in Eqs. (6)–(8) do not depend on the chemical term R, and the results of this work are valid for any chemical front.

CONCLUSION

In this paper, we solve numerically the hydrodynamic equations governing the evolution of the exothermic Fisher front. We observe two qualitatively different behaviors depending on whether the reaction front propagates sufficiently faster or slower than the sound speed at the initial temperature. For a large velocity the reaction front propagates to the unperturbed steady state with the marginal velocity U_0 of the isothermal case. For a small velocity the heat front precedes the reaction front and positive deviations from U_0 appear. A gap of reaction front velocities around the sound speed is observed when the activation energy is continuously increased. We analytically prove the existence of a forbidden interval of reaction front velocities for which traveling fronts cannot exist. The length of this interval increases with the heat of the reaction.

ACKNOWLEDGMENTS

We wish to acknowledge the support of the program Polonium 09376SF and the joint project 14491 between CNRS (France) and the Polish Academy of Sciences.

[1] R. A. Fisher, Ann. Eugenics **7**, 355 (1937).
[2] A. N. Kolmogorov, I. G. Petrovsky, and N. S. Piskunov, Bull. Moscow State Univ. Math. and Mechanics **1**, 1 (1937).
[3] W. van Saarloos, Phys. Rev. Lett. **58**, 2571 (1987).
[4] E. Brunet and B. Derrida, Phys. Rev. E **56**, 2597 (1997).
[5] D. Panja, Phys. Rep. **393**, 87 (2004).
[6] D. A. Frank-Kamenetskii, *Diffusion and Heat Exchange in Chemical Kinetics* (Princeton University Press, Princeton, NJ, 1955).
[7] Y. B. Zeldovich, G. I. Barenblatt, V. B. Librovich, and G. M. Makhviladze, *The Mathematical Theory of Combustion and Explosions* (Plenum, New York, 1985).
[8] D. Campos, J. E. Llebot, and J. Fort, J. Phys. A **37**, 6609 (2004).
[9] G. I. Sivashinsky, Acta Astronaut. **4**, 1177 (1977).
[10] P. Clavin, Prog. Energy Combust. Sci. **11**, 1 (1985).
[11] O. Colin, F. Ducros, D. Veynante, and T. Poinsot, Phys. Fluids **12**, 1843 (2000).
[12] J. Riordan, C. R. Doering, and D. ben-Avraham, Phys. Rev. Lett. **75**, 565 (1995).
[13] J. Mai, I. M. Sokolov, and A. Blumen, Europhys. Lett. **44**, 7 (1998).
[14] A. Lemarchand and B. Nowakowski, Europhys. Lett. **41**, 455 (1998).
[15] A. Lemarchand and B. Nowakowski, J. Chem. Phys. **109**, 7028 (1998).
[16] A. Lemarchand and B. Nowakowski, J. Chem. Phys. **111**, 619 (1999).
[17] C. R. Doering, C. Mueller, and P. Smereka, Physica A **325**, 243 (2003).
[18] J. G. Conlon and C. R. Doering, J. Stat. Phys. **120**, 421 (2005).
[19] J. S. Hansen, B. Nowakowski, and A. Lemarchand, J. Chem. Phys. **124**, 034503 (2006).
[20] J. S. Hansen, B. Nowakowski, and A. Lemarchand, J. Chem. Phys. **125**, 044313 (2006).
[21] D. A. McQuarrie, *Statistical Mechanics* (Harper and Row, New York, 1976).
[22] E. Salomons and M. Mareschal, Phys. Rev. Lett. **69**, 269 (1992).
[23] V. Bychkov, A. Petchenko, V. Akkerman, and L.-E. Eriksson, Phys. Rev. E **72**, 046307 (2005).
[24] S. Kadowaki, H. Suzuki, and H. Kobayashi, Proc. Combust. Inst. **30**, 169 (2005).
[25] Y. B. Zel'dovich and Y. P. Raizer, *Physics of Shock Waves and High-Temperature Hydrodynamics Phenomena* (Academic, New York, 1966).
[26] B. Lucas, G. Gregoire, J. Lemaire, P. Maitre, J. M. Ortega, A. Rupenyan, B. Reimann, J. P. Schermann, and C. Desfrancois, Phys. Chem. Chem. Phys. **6**, 2659 (2004).
[27] M. Guisnet, P. Andy, N. S. Gnep, E. Benazzi, and C. Travers, Oil Gas Sci. Technol. **54**, 23 (1999).